In vivo functional photoacoustic microscopy of cutaneous microvasculature in human skin

Christopher P. Favazza,ª Lynn A. Cornelius,ᵇ and Lihong V. Wangª
ªWashington University in St. Louis, Optical Imaging Laboratory, Department of Biomedical Engineering, One Brookings Drive, Campus Box 1097, St. Louis, Missouri 63130
ᵇWashington University School of Medicine, Division of Dermatology, 660 S. Euclid, Campus Box 8123, St. Louis, Missouri 63110

Abstract. Microcirculation is an important component of the cardiovascular system and can be used to assess systemic cardiovascular health. Numerous studies have investigated cutaneous microcirculation as an indicator of cardiovascular related diseases. Such research has shown promising results; however, there are many limitations regarding the employed measurement techniques, such as poor depth and spatial resolution and measurement versatility. Here we show the results of functional cutaneous microvascular experiments measured with photoacoustic microscopy, which provides high spatial resolution and multiparameter measurements. In a set of experiments, microvascular networks located in the palms of volunteers were perturbed by periodic ischemic events, and the subsequent hemodynamic response to the stimulus was recorded. Results indicate that during periods of arterial occlusion, the relative oxygen saturation of the capillary vessels decreased below resting levels, and temporarily increased above resting levels immediately following the occlusion. Furthermore, a hyperemic reaction to the occlusions was measured, and the observation agreed well with similar measurements using more conventional imaging techniques. Due to its exceptional capability to functionally image vascular networks with high spatial resolution, photoacoustic microscopy could be a beneficial biomedical tool to assess microvascular functioning and applied to patients with diseases that affect cardiovascular health. © 2011 Society of Photo-Optical Instrumentation Engineers. © *2011 Society of Photo-Optical Instrumentation Engineers (SPIE)*. [DOI: 10.1117/1.3536522]

Keywords: photoacoustic microscopy; hemodynamics; reactive hyperemia; microcirculation; skin.

Paper 10470R received Aug. 24, 2010; revised manuscript received Nov. 11, 2010; accepted for publication Dec. 7, 2010; published online Feb. 7, 2011.

1 Introduction

Predictive medicine is a growing field, garnering an increasing amount of interest and research. It holds the potential to identify the risk or early onset of diseases, thereby enabling better treatment or even prevention of a disease. As an example, microcirculatory systems have been investigated for the potential to provide clinical insight regarding cardiovascular related diseases. Cardiovascular diseases are major contributors to mortality and morbidity globally, and account for a large portion of healthcare costs.[1–4] Numerous diseases have sequelae that adversely affect the microcirculation, including diabetes mellitus, coronary artery disease, hypertension, atherosclerosis, arteriosclerosis, and peripheral vascular disease.[2] Young diabetes patients have documented measurable, functional changes in skin microvasculature long before clinical evidence of vascular disease.[5]

The cutaneous microvascular network of the extremities has proven to be an valuable and measurable site due to the concentration of superficial vasculature and ease of access. Furthermore, circulation through these vessels can be readily manipulated to determine response to injury or "insult," thereby eliciting reproducible measurements both intra- and inter-individually. One technique is to induce an ischemic event by occluding blood flow in larger vessels "upstream." Upon releasing the temporary occlusion, reactive hyperemia results from post-ischemic vessel

dilation. It has been suggested that evaluation of reactive hyperemia could be a clinically relevant diagnostic measure.[1,6–9] The regulation system that controls vessel dilation and blood flow in healthy subjects can dramatically increase perfusion by more than ten times the value during resting flow conditions. However, in subjects with peripheral arterial occlusive disease (PAOD), this capability is measurably reduced.[6–10] Likewise, it has been shown that the recovery from a hyperemic state to resting conditions is prolonged in patients with PAOD.[7]

Several other studies have shown differences in oxygen consumption and rates of change in oxygen saturation (sO_2) between healthy and diseased (peripheral vascular disease) volunteers,[1,5,8,11,12] and a near-infrared (NIR) spectroscopy based diagnostic test has been patented.[9] Typically, changes in perfusion from post-occlusive reactive hyperemia (PORH) are measured with laser Doppler flowmetry,[2,6,7,13] and oxygen saturation measurements are obtained with near-infrared spectroscopy.[1,5,8,11,12] While both techniques have successfully measured repeatable and quantifiable parameters during PORH, they are inherently limited by poor spatial resolution and versatility (i.e., number of different measurements). Currently, there is no gold standard measurement technique.

Recent studies have demonstrated the unparalleled vascular imaging capabilities of photoacoustic microscopy (PAM). It has been well established that PAM can effectively and noninvasively measure sO_2 and total amounts of hemoglobin in vascular

Address all correspondence to: Lihong V. Wang, Washington University in St. Louis, Optical Imaging Laboratory, Department of Biomedical Engineering. Email: lhwang@wustl.edu.

networks *in vivo*.[14,15] Additionally, PAM can be used to measure blood flow[16] and vasodilation and vasomotion in response to external stimuli.[17,18] All of the aforementioned measurements are obtained while concurrently imaging the vessels being probed, yielding specific information about individual vessels. Whereas most previous hemodynamic studies using PAM have been limited to animal models, here we show its application to microcirculation in humans in which the microvascular response to periodic arterial occlusions in different volunteers was photoacoustically imaged. Relative changes in sO$_2$ and capillary perfusion were measured and showed drastic changes due to the occlusions. The results indicate that PAM could be a valuable tool to monitor and assess cutaneous microvascular functioning. Unlike more conventional measurement techniques, PAM has the potential to provide more information from single datasets with such information attributed to individual blood vessels.

2 Methods

2.1 *PAM*

A dark-field photoacoustic microscope built by our laboratory[19] was employed to image the microvascular response to periodic occlusions of the brachial artery in five different volunteers. Figure 1 shows a photograph of the microscope as it was used in the described experiment along with a schematic of the entire system. An Nd:YLF laser pumped a wavelength tunable dye laser, which supplied the optical energy for the PAM. The laser beam had a pulse width less than 5 ns and operated at a ~1 kHz repetition rate, which depended on scanning parameters, such as motor speed and step size. A fiber optic cable routed and coupled the laser beam to the scan head of the PAM. The beam passed through a conical lens and was weakly focused with a condensing lens, forming a dark-field illumination pattern on the surface of the target. For this experiment, we used a focused broadband single element ultrasound transducer with a 20 MHz central frequency and 0.61 NA. With this configuration, the PAM can achieve 70 μm lateral resolution and 54 μm axial resolution.[20] Using Rhodamine 6G dye, we generated laser light at 561 and 570 nm wavelengths to image the volunteers.

2.2 *Volunteers*

In this study, we investigated cutaneous microvascular networks in the palms of the volunteers. This study was approved by the Human Research Protection Office of Washington University
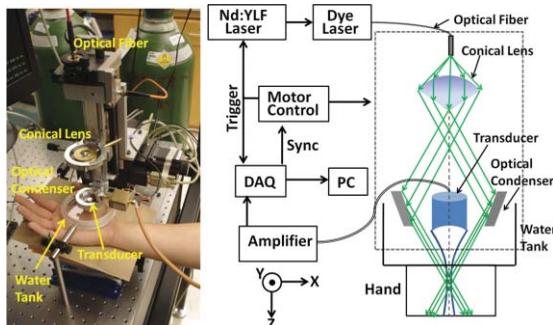
(09–0270). For each volunteer both "static" three-dimensional (3D) and "dynamic" functional images were acquired. As part of the imaging protocol, ultrasonic gel was spread on the palm of the volunteer, which was then directly placed in acoustic contact with the thin plastic membrane that formed the bottom of the water tank that housed the ultrasound transducer. First, two three-dimensional images were acquired at laser wavelengths of 561 and 570 nm. An area of 8 $\times$ 4 mm^2 was scanned, and the total acquisition was completed within approximately 10 min. A surface laser fluence of ~2 mJ/cm^2 was incident on the skin of the volunteers. This fluence value is well below the maximum permissible exposure (MPE) limit governed by the American National Standards Institute, which limits exposure to ~5.8 mJ/cm^2 for these experiments.[21] The preceding MPE limit represents the corrected value, which compensates for repetitive pulses generated from raster scanning.[21] However, the Center for Devices and Radiological Health in the Food and Drug Administration does not recognize this correction factor to evaluate laser safety, which would limit the exposure to 20 mJ/cm^2 (Refs. 21 and 22).

Following image acquisition, the data was quickly displayed, and a specific cross-section was chosen from the dataset for functional imaging. The cross-section was selected based on the presence of deeper vessels in the field of view. The selected cross-section was then repeatedly imaged at both laser wavelengths over the course of 15 min at 15 s intervals. During this monitoring period, two ischemic events were induced by inflating a common arm cuff to a standard pressure of ~280 mm Hg for each volunteer to ensure an arterial occlusion. This pressure was maintained for 3 min, and each occlusion was initiated after 3 and 9 min into the scan. There was approximately 1 s between each B-scan image for both wavelengths, due to the time required to mechanically tune the laser wavelength.

3 Results and Discussion

In the first portion of the experiment, two 3D images were acquired at two different laser wavelengths. Figure 2(a) shows a representative maximum amplitude projection (MAP) of a typical 3D image. The MAP shows the blood vessels imaged at an isosbestic point for hemoglobin, a wavelength where the molar optical absorption coefficients of both oxy and deoxyhemoglobin (HbO$_2$ and HbR) are equivalent. During the construction of the MAP, a signal from the epidermis and epidermal-dermal junction, including capillaries, was removed to better display the sub-papillary plexus below it. The capillary vessels were removed because they cannot be resolved, given the resolution of this PAM, and would cloud the MAP with a diffuse signal. However, it is possible to resolve capillary vessels with higher resolution PAMs.[23–25] The dashed line in the MAP image [Fig. 2(a)] indicates the cross-section or B-scan that was selected to be monitored during the periodic arterial occlusions, shown in Figs. 2(b)–2(d).

During the functional imaging portion of the experiment, there were clear changes in the Photoacoustic (PA) signal during and after the release of the occlusion, as compared to the signal obtained during the initial resting period. The changes are clearly illustrated in Figs. 2(b)–2(d) and 3. Figures 2(b)–2(d) show B-scans acquired before [Fig. 2(b)], during [Fig. 2(c)], and after [Fig. 2(d)] the occlusion. Each image is plotted on the same color
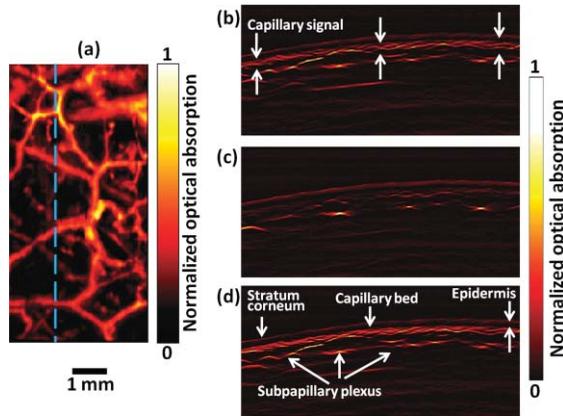

Fig. 1 Photograph and schematic of the photoacoustic microscope. (Color figures available online only.)

Fig. 2 (a) Maximum amplitude projection of a coarse 3D photoacoustic image taken from the palm of a volunteer. The bright areas in the image show the photoacoustic signal generated from the volunteers' blood vessels. The blue dashed line indicates the cross-section selected for functional imaging shown in Figs. 2(b)–2(d). (b) B-scan of the monitored cross-section before the blood flow was occluded. (c) B-scan during the occlusion. (d) B-scan acquired after the occlusion. The scale bar below (a) applies to all images in Fig. 2. (Color figures available online only.)

scale, and as shown in the images, there is a drastic reduction of signal during the occlusion and increase in signal after the occlusion. The PA signal, particularly at an isosbestic wavelength, is directly proportional to the total amount of hemoglobin (i.e., total amount of blood) in a given vessel. Hence these images show a decrease and increase in perfusion during and after ischemia, respectively.

A representative experiment for a single volunteer is shown pictorially in MAPs in Figs. 3(a)–3(b). These MAPs were constructed in a similar fashion to the MAP shown in Fig. 2(a), except that the unresolved capillaries in the epidermal–dermal junction were included in the projection. Also, these MAPs are projections of a single cross-section with B-scans acquired at different times, so the left-hand edge of the MAP shows the first
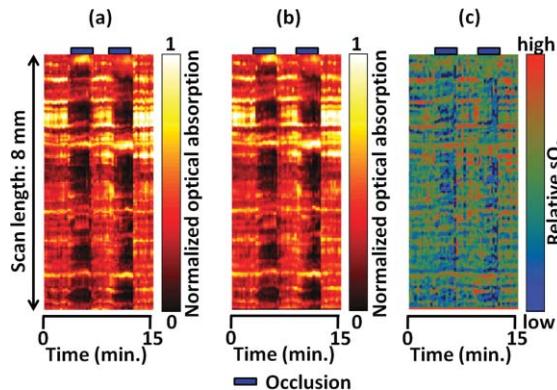
acquired B-scan and the right-hand side shows the last B-scan collected 15 min later. In these images, there is an obvious reduction in the PA signal strength during the occlusions. Less clear is the increase in signal after release of the occlusion, but it is easily measured. Figure 3(c) shows the ratio of the two MAPs, the MAP obtained at 561 nm divided pixel-by-pixel by the MAP collected at 570 nm. HbR has a relative absorption peak at 561 nm, making light at this wavelength HbR absorption dominant. This ratio of signal collected at an HbR peak to signal collected at an isosbestic point indicates relative changes in the concentration of HbR. The ratio, shown in Fig. 3(c), reveals lower oxygen saturation levels during ischemia.

For more quantitative analysis, PA signals from the capillary vessels were integrated for each B-scan. A representative selected area of capillary vessels is shown in between the indicator arrows in the B-scan in Fig. 2(b). The plot depicted in Fig. 4 shows the relative change in the ratio of the PA signals acquired with 561 and 570 nm. A baseline measurement was determined by averaging the measurements acquired before either occlusion, and the relative changes in the data were calculated from this baseline measurement. All five volunteers consistently showed a strong response to the arterial occlusions, where the relative concentration of HbR rose after the onset of ischemia (Fig. 4). Also, immediately following the release of the occlusion there was a relative decrease in HbR concentration, which quickly began to approach resting conditions during the period
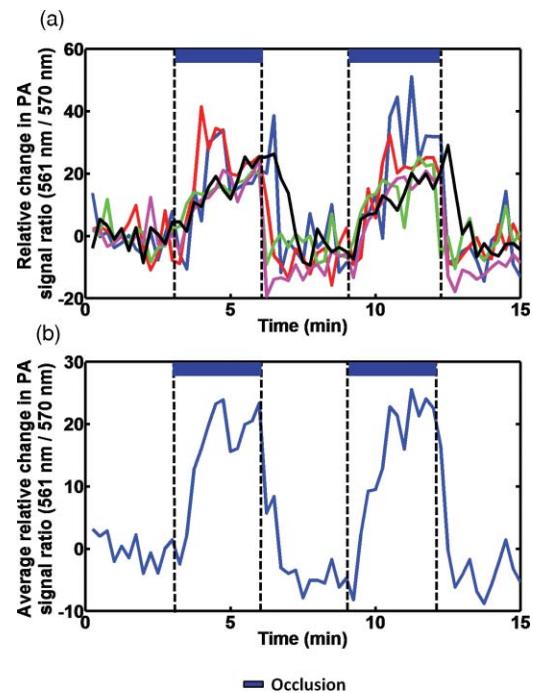

Fig. 3 MAPs of each B-scan at every time point during the experiment. (a) The MAP of the data collected with 570 nm laser light and (b) the MAP acquired at 561 nm both show a reduction in the photoacoustic signal during the occlusion periods, as indicated by the blue boxes on the side of the images. (c) The ratio between the MAPs collected at different laser wavelengths (561 nm/570 nm). The increase of the darker regions (blue online) in the image during the occlusion periods show the relative increase in deoxyhemoglobin concentration. (Color figures available online only.)

Fig. 4 Plots of the relative change in the photoacoustic signal generated from the capillary bed of each of the five volunteers. The ratio of the signal collected at 561 nm (a deoxyhemoglobin local maximum) and 570 nm (an isosbestic wavelength) indicates the relative change in the concentration of deoxyhemoglobin in the vessels. The measured relative deoxyhemoglobin concentration increases during the occlusions (marked by the boxes at the top of the plots (blue online)) and drops below the resting level immediately following the occlusion. (a) Individual data from each volunteer. (b) Averaged data for all five volunteers. (Color figures available online only.)

of free flow. The average maximum relative increase in HbR for all volunteers was 20.3 ± 3.8% and 21.3 ± 8.1% for the first and second occlusions, respectively. The average maximum relative decrease in HbR (from resting conditions) for all volunteers was 5.6 ± 2.7% and 4.3 ± 4.0% for the first and second occlusions, respectively. These results are consistent with results from de Mul et al., who indirectly examined the ratio of the oxygen debt incurred during the occlusion to the oxygen recouped following the occlusion.[7] This ratio was found to be less than unity for healthy volunteers,[7] which is consistent with the relative sO$_2$ measurements yielded by PAM.

Directly following the release of the occlusion, a significant increase in signal strength was observed, signifying the reactive hyperemic response. There have been numerous studies investigating PORH as a measure of vascular functioning and health. Previous PORH measurements have been acquired with different techniques, such as near-infrared spectroscopy, laser Doppler flowmetry, and strain gauge plethysmography. de Mul et al. used laser Doppler to measure changes in perfusion of cutaneous microvasculature located in the extremities of volunteers of both healthy and PAOD patients, and presented a model of blood flow through cutaneous capillary networks.[7] This compartmental model of the microvascular system describes blood flow through the capillaries as related to vascular functions (i.e., local perfusion of vessels) and its simplified form is expressed as the following:

$$I(t) = I_r[1 - \exp[(-t/\tau_1)]*[1 + (\rho_{m-}1)\exp(-t/\tau_2)];$$

where ρ_m is the ratio of the maximum perfusion during hyperemia to the normal resting condition; τ_1 and τ_2 are decay constants for arteriole and capillary vessels; $I(t)$ and I_r are time-dependent and resting blood flow; and t is time.[7]

de Mul et al. found common values of τ_1 and τ_2 for healthy individuals based on the assumption that the blood flow is proportional to the measured perfusion of flux.[7] PAM measures relative total amounts of hemoglobin or blood volume. However, the described model is predicated on time-varying resistance of capillaries due to filling, and arteriole time-varying-resistance due to vasodilation. In essence, it is assumed that temporal changes of flow are directly related to temporal changes in the blood volume of the arterioles and capillaries, both of which are measured by PAM. Consequently, we have applied this model in healthy human volunteers to the time-varying PA signal acquired at 570 nm, a measure of the relative total blood volume.

Figure 5 shows volunteer data and the fit with the model, using the time constants found for healthy individuals by de Mul et al. Using the published time constants, the data fit the model well with coefficient of determination, R^2, values of 0.92 and 0.95 for each ischemic event. ρ_m, the ratio of the maximum PA signal during hyperemia to the PA signal during resting conditions, was used as a fitting parameter to achieve the best fit, justified by the fact that the actual peak PA signal may have been missed due to the time interval between successive scans. However, the fitted value of ρ_m was within 5% of the calculated value. Also, due to the coarse time steps of the measurements and the manual occlusion release mechanism used in the experiment, a time point within several seconds of the lowest PA signal was taken as the "time-zero" point of the hyperemic model.
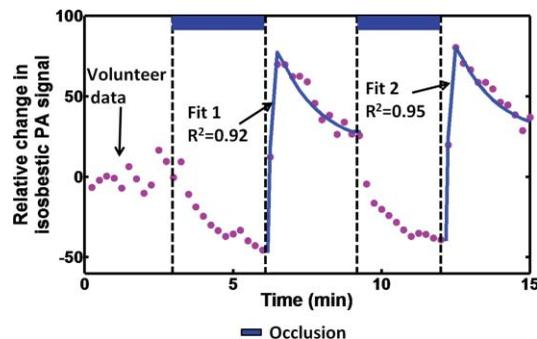

Fig. 5 Plot of the relative change in the photoacoustic signal acquired at the isosbestic wavelength (570 nm) for oxy and deoxyhemoglobin. Changes in the photoacoustic signal at this wavelength show changes in hematocrit in the vessel, corresponding to the total amount of blood in the vessel. During the occlusion (blue boxes), the amount of blood decrease; immediately following the occlusions, the vessels enter hyperemic state. The curve fitting for both hyperemia states utilized a previously published model of reactive hyperemia (Ref. 7) and the reported time constants for healthy individuals. (Color figures available online only.)

These results demonstrate the feasibility of using PAM to assess microvascular functioning in normal healthy human volunteers. We recognize that to evaluate the diagnostic potential of PAM, we will need to apply this technology to populations having specific disease diagnoses, such as diabetes and hypertension. Moreover, a PAM system tailored for clinical imaging will enhance its utility and acceptance in a clinical setting. Specifically, leveraging the advancements made in PA image acquisition speed will reduce the time required to collect a 3D image and improve image quality and patient comfort. Also, a microvascular PORH diagnostic or assessment test could be much shorter than the 15 min spent in these experiments. For instance, by measuring a single PORH event and collecting a shorter baseline measurement, a clinical PORH test could require less than half the time spent in the presented functional imaging experiments. Further studies utilizing faster and higher resolution PAM with these cohorts are currently in progress.

4 Conclusion

PAM was proven effective at monitoring hemodynamic changes induced by periodic arterial occlusions in cutaneous microvascular networks in human volunteers. Specifically, PAM measurements showed a relative decrease in sO$_2$ during ischemia and a slight relative increase in sO$_2$ post-occlusion. Also, PAM obtained time-resolved measurements of PORH that matched well with previously published data and existing theoretical models. These results suggest that PAM could be a useful clinical tool providing multiparameter measurements to characterize the microcirculation—potentially aiding in disease diagnosis, the prediction of disease sequelae, and the evaluation of therapeutic interventions in patients with diseases that affect cardiovascular functioning.

5 Conflict of Interest

References

1. R. Kragelj, T. Jarm, T. Erjavec, M. Presern-Strukeij and D. Miklavcic, "Parameters of postocclusive reactive hyperemia measured by near infrared spectroscopy in patients with peripheral vascular disease and in healthy volunteers," *Ann. Biomed. Eng.* **29**(4), 311–320 (2001).
2. G. B. Yvonne-Tee, A. H. Rasool, A. S. Halim, and A. R. Rahman, "Noninvasive assessment of cutaneous vascular function in vivo using capillaroscopy, plethysmography and laser-Doppler instruments: its strengths and weaknesses," *Clin. Hemorheol. Microcirc.* **34**(4), 457–473 (2006).
3. J. Leal, R. Luengo-Fernandez, A. Gray, S. Petersen, and M. Rayner, "Economic burden of cardiovascular diseases in the enlarged European Union," *Eur. Heart J.* **27**(13), 1610–1619 (2006).
4. R. Luengo-Fernandez, J. Leal, A. Gray, S. Petersen, and M. Rayner, "Cost of cardiovascular diseases in the United Kingdom," *Heart* **92**(10),1384–1389 (2006).
5. F. Khan, T. A. Elhadd, S. A. Greene, and J. J. Belch, "Impaired skin microvascular function in children, adolescents, and young adults with type 1 diabetes," *Diabetes Care* **23**(2), 215–220 (2000).
6. G. Addor, A. Delachaux, B. Dischi, D. Hayoz, L. Liaudet, B. Waeber, and F. Feihl, "A comparative study of reactive hyperemia in human forearm skin and muscle." *Physiol. Res.* **57**(5), 685–692 (2008).
7. F. F. de Mul, F. Morales, A. J. Smit, and R. Graaff, "A model for post-occlusive reactive hyperemia as measured with laser-Doppler perfusion monitoring," *IEEE Trans. Biomed. Eng.* **52**(2), 184–190 (2005).
8. T. R. Cheatle, L. A. Potter, M. Cope, D. T. Delpy, P. D. Coleridge Smith, and J. H. Scurr, "Near-infrared spectroscopy in peripheral vascular disease," *Br. J. Surg.* **78**(4) 405–408 (1991).
9. J. J.-m Mao, *Diagnosing peripheral vascular disease by monitoring oxygen saturation changes during a hyperemia phase*, Fremont, CA, United States (2009).
10. A. K. Andreassen, K. Kvernebo, B. Jorgensen, S. Simonsen, J. Kjekshus, and L. Gullestad, Exercise capacity in heart transplant recipients: relation to impaired endothelium-dependent vasodilation of the peripheral microcirculation, *Am. Heart J.* **136**(2), 320–328 (1998).
11. X. Cheng, J. M. Mao, X. Xu, M. Elmandira, R. Bush, L. Christenson, B. O'Keefe, and J. Bry, "Post-occlusive reactive hyperemia in patients with peripheral vascular disease," *Clin. Hemorheol. Microcirc.* **31**(1), 11–21 (2004).
12. R. Kragelj, T. Jarm, and D. Miklavcic, "Reproducibility of parameters of postocclusive reactive hyperemia measured by near infrared spectroscopy and transcutaneous oximetry," *Ann. Biomed. Eng.* **28**(2), 168–173 (2000).
13. A. Kruger, J. Stewart, R. Sahityani, E. O'Riordan, C. thompson, S. Adler, R. Garrick, P. Vallance and M. S. Goligorsky, "Laser Doppler flowmetry detection of endothelial dysfunction in end-stage renal disease patients: correlation with cardiovascular risk, "*Kidney Int.* **70**(1), 157–164 (2006).
14. E. W. Stein, K. Maslov, and L. V. Wang, "Noninvasive, in vivo imaging of blood-oxygenation dynamics within the mouse brain using photoacoustic microscopy," *J. Biomed. Opt.* **14**(2), 020502 (2009).
15. H. F. Zhang, K. Maslov, G. Stoica and L. V. Wang, "Functional photoacoustic microscopy for high-resolution and noninvasive *in vivo* ima*ging*," *Nat. Biotechnol.* **24**(7), 848–851 (2006).
16. J. Yao, K. I. Maslov, Y. Shi, L. A. Taber and L. V. Wang, "*In vivo* photoacoustic imaging of transverse blood flow by using Doppler broadening of bandwidth," *Opt. Lett.* **35**(9),1419–1421.
17. S. Hu, K. Maslov, V. Tsytsarev and L. V. Wang, "Functional transcranial brain imaging by optical-resolution photoacoustic microscopy," *J. Biomed. Opt.* **14**(4), 040503 (2009).
18. S. Hu, K. Maslov, and L. V. Wang, "Noninvasive label-free imaging of microhemodynamics by optical-resolution photoacoustic microscopy," *Opt. Express* **17**(9), 7688–7693 (2009).
19. K. Maslov, G. Stoica, and L. V. Wang, "*In vivo* dark-field reflection-mode photoacoustic microscopy," *Opt. Lett.* **30**(6), 625–627 (2005).
20. E. W. Stein, K. Maslov, and L. V. Wang, "Noninvasive, *in vivo* imaging of the mouse brain using photoacoustic microscopy, "*J. Appl. Phys.* **105**(10), 102027 (2009).
21. *American National Standard for Safe Use of Lasers (ANZI Z136.1–2000)*, American National Standards Institute, New York (2000).
22. http://www.osha.gov/dts/osta/otm/otm_iii/otm_iii_6.html.
23. S. Hu, K. Maslov, and L. V. Wang, "*In vivo* functional chronic imaging of a small animal model using optical-resolution photoacoustic microscopy," *Med. Phys.* **36**(6), 2320–2323 (2009).
24. K. Maslov, H. F. Zhang, S. Hu, and L. V. Wang, "Optical-resolution photoacoustic microscopy for *in vivo* imaging of single capillaries," *Opt. Lett.* **33**(9), 929–931 (2008).
25. J. Yao, K. Maslov, S. Hu, and L. V. Wang, "Evans blue dye-enhanced capillary-resolution photoacoustic microscopy *in vivo*," *J. Biomed. Opt.* **14**(5), 054049 (2009).